

Optical Engineering

SPIDigitalLibrary.org/oe

Movement layout and adjustment for a specialized video measuring system

Xinbo Liu
Zhong Wang
Jigui Zhu
Jin Zhang

Movement layout and adjustment for a specialized video measuring system

Xinbo Liu

Zhong Wang

Jigui Zhu

Tianjin University

State Key Laboratory of Precision Measuring

Technology and Instruments

Tianjin 300072, China

E-mail: liu33-33xinbo@163.com

Jin Zhang

Hefei University of Technology

School of Instrument Science and

Opto-Electronics Engineering

Anhui 230009, China

Abstract. Specialized video measuring system (SVMS) is a kind of instruments diagnosing only one special type of part with high performance. In the design of a SVMS, it is necessary to consider the special requirements during the inspection of the parts. We take the video-based inspecting instrument for watch escapement (VIIWE) as an example of SVMS. A method based on least interferences is proposed to determine an optimized movement layout. The quality of image taken by an imaging lens with a limited depth of field ($100\ \mu\text{m}$) may be degraded by two parameters, i.e., the perpendicularity of optical axis to workbench and the parallelism of probe movement plane to workbench. To optimize the two parameters, we calibrate the perpendicularity with a definition function, measure the parallelism with a dial indicator, and develop a mechanism of adjustment. The scheme about movement layout and adjustment has been successfully applied in the VIIWE. © 2012 Society of Photo-Optical Instrumentation Engineers (SPIE). [DOI: [10.1117/1.OE.51.8.081513](https://doi.org/10.1117/1.OE.51.8.081513)]

Subject terms: movement layout; perpendicularity; parallelism; video measuring system; depth of field; adjustment.

Paper 111042SSP received Aug. 28, 2011; revised manuscript received Nov. 24, 2011; accepted for publication Dec. 28, 2011; published online May 22, 2012.

1 Introduction

Manufacturers have developed various types of video measuring instruments with high accuracy. However, these instruments are developed based on a “point to point” mode like a microscope to measure different workpieces.¹ Due to this low-efficiency work mode, it cannot meet the requirements of detecting a single type of parts in large volumes. Consequently, an instrument termed specialized video measuring system (SVMS) has been taken into consideration. It is designed for a single type of workpiece with a higher accuracy and a higher speed than most conventional video measuring systems (CVMS). For example, one type of SVMS, the video-based inspecting instrument for watch escapement (as shown in Fig. 1) has the following characteristics: (1) A camera with a resolution of 2048×2048 pixels captures images of the entire escapement at one shot, and a telecentric lens is designed to keep aberrations as small as possible especially near the edge of the escapement, where most geometric parameters distribute. Integrating the camera and the lens ensures the measuring error is less than $3\ \mu\text{m}$ in an area of 7.4-mm diameter. (2) A novel feed system of placing an array of 6×10 escapements and a precise motion control system are used to achieve a continuous and automatic measurement of the workpieces.² The characteristics of the video-based inspecting instrument for watch escapement (VIIWE) can help to reduce the times of photographing and improve detector-positioning speed. Therefore, the SVMS is a feasible solution for the measurements of large-volume parts with a high accuracy.

Movement layout is about determining whether the workbench or the shooting component acts as an active one in each axis, since most video measuring systems should be enabled

to keep the camera moving relative to workbench multidirectionally. In general, a good movement layout can optimize its structures and functions. The design of a CVMS always follows a traditional rule of mechanical design called “moving the lighter.” It means the lighter one will be assigned as the moving part after comparing the weight of the workbench and the shooting component. For example, the CNC-250 (OGP Corp, Rochester, State of New York) moves the shooting component because it is lighter than the workbench, while the CNC-600 moves the workbench for it weighs less. This rule is useful for a system to measure various objects with more portable structure. However, a lot of problems will occur if we still insist on this rule when a part is measured with particular requirements. A problem is encountered in the design of VIIWE. The workbench is lighter than the shooting component. Nevertheless, if the workbench is moved horizontally, other requirements, such as arranging the workpieces as an array and keeping each of them in the field of view when they are being measured, will not be satisfied. Therefore, we investigate different SVMS layouts, and choose the best one for the VIIWE.

In addition, it is well known that image sharpness mainly depends on whether the workpiece is within the depth of field or not. Then, another problem occurs in the design of VIIWE. In order to save the system’s adjusting time, focusing is not recommended when a group of workpieces on the workbench of the VIIWE are measured respectively and automatically. The similar magnification for every sharp image allows very slight changes in the object distance when the camera moves relative to an object. So the proper lens should be telecentric and have only a depth of field of $100\ \mu\text{m}$ by the formulas in Leslie’s view camera technique.^{3,4} The range is rather narrow; however, several factors result in the distance between lens and the measured object changing, such as the perpendicularity of optical axis to

workbench and the parallelism of probe movement plane to workbench. As a result, the allowed range for each factor is narrower. To meet such a requirement, an adjustment method is developed to limit errors in both parallelism and perpendicularity.

Some studies have been done for the layout of SVMS. Chen and Li have designed a method of automatic sensor placement for model-based robot vision, which allows three-dimensional (3-D) images to be taken from different vantages of viewpoints.⁵ Scott has developed a multi-phase, model-based approach to view planning for an automated, high fidelity object inspection or reconstruction by means of laser scanning range sensors.⁶ Most of the previous studies emphasize on the vision sensor planning while few of them can be referred to the movement parts' layout. Meanwhile, there are many classic methods on the adjustment technology in SVMS.⁷⁻⁹ For example, Ryoo and Doh estimate the deviated neutral position of the objective lens from the optical axis by the power intensity of a laser spot and then add pulses to the driving input of a fine actuator to align the objective lens to the optical axis. This method has the advantages of convenience, simpleness, and real time, but it only works well in a short measuring distance, and its accuracy is not high enough for the measurement at micron scale. We have to admit not such a perfect adjustment scheme which is available for all types of SVMS. Different adjustment methods need to be adopted according to different requirements.

The remainder of the paper is divided into five sections. In Sec. 2, after having reviewed the movement layouts of SVMS, we introduce how to choose a layout for VIIWE. Section 3 details the factors of changing the object distance. The design of the adjustment scheme is described in the Sec. 4. The whole design, the phases of adjustment, and the experimental results are shown in the Sec. 5. Section 6 summarizes our results.

2 Movement Layout for Video-Based Inspecting Instrument for Watch Escapement

The visual detector in a video-based measurement system usually works with two motions: photographing and feeding.¹⁰ Photographing, completed by a command from the computer to trigger the camera shutter, is almost irrelevant to the structure of the instrument. However, feeding, which is a relative motion between the camera and the workbench, is completed by corresponding executive components that compose the main structure of the instrument. Therefore, choosing the workbench or the shooting component as a moving part in each direction becomes the main problem in designing the movement layout.

As shown in Fig. 2, there will be eight layout solutions in total supposing all feeding movements of the instrument distributed in x -, y -, and z -directions are linear. If the rotational motion or more linear movements are considered, there would be more layout forms which are not required for the VIIWE and therefore will not be discussed further in this paper.

The tested object in the VIIWE is the escape wheel of a mechanical watch as shown in Fig. 3. Both the escape wheel and the workbench carrying objects are lighter than the shooting component that is composed of a camera, a lens, and holders. Thus, the layout form as shown in Fig. 2(a)



Fig. 1 Video-based inspecting instrument for watch escapement (VIIWE).

should be chosen if we obey the rule of mechanism design, moving the lighter.¹⁰ However, capturing the image of escapement entirely at one shot requires the upper surface of the tested object uncovered. If the scheme in Fig. 2(a) was applied, it would be rather difficult to mount the tested object properly because the gripping mechanism could damage the integrity of an image. Furthermore, placing the tested objects freely would damage the stability of the array type due to the acceleration when the workbench starts or stops. The layouts in Fig. 2(d)–2(f) have the same drawbacks as in Fig. 2(a). Only ones in Fig. 2(g) and 2(h) could meet the requirements of placing the tested object freely and regularly while keep the workbench stationary in the horizontal plane. The layout in Fig. 2(g) is eventually used. It obeys the rule of moving the heavier in the x and y directions while only keeping the conventional designing concept of moving the lighter in the z direction. This type of movement layout also benefits the perpendicularity between the optical axis and the object plane, which will be discussed later.

3 Error Analysis

Generally, it is necessary to pre-determine whether the image is clear enough for the imaging to progress. The defocus of the system is limited to $\pm 5 \mu\text{m}$ by using the square gradient image definition evaluation function.^{3,11} The total error along the optical axis cannot exceed $90 \mu\text{m}$ due to the restriction of only $100 \mu\text{m}$ in the depth of field. Actually, both the 3-D movement errors and the original assembly error will result in a change of the object distance.¹² The 3-D movement errors can be divided into the error of parallelism between probe movement plane and workbench and the error in the straight, vertical motion. The original assembly error can be regarded as the error of perpendicularity between optical axis and workbench.

3.1 Perpendicularity Analysis

When the optical axis is not perpendicular to the workbench, a circle will be imaged as an ellipse because most lenses can only focus on the frontal parallel plane. Therefore, the deviation angle between the optical axis of the shooting

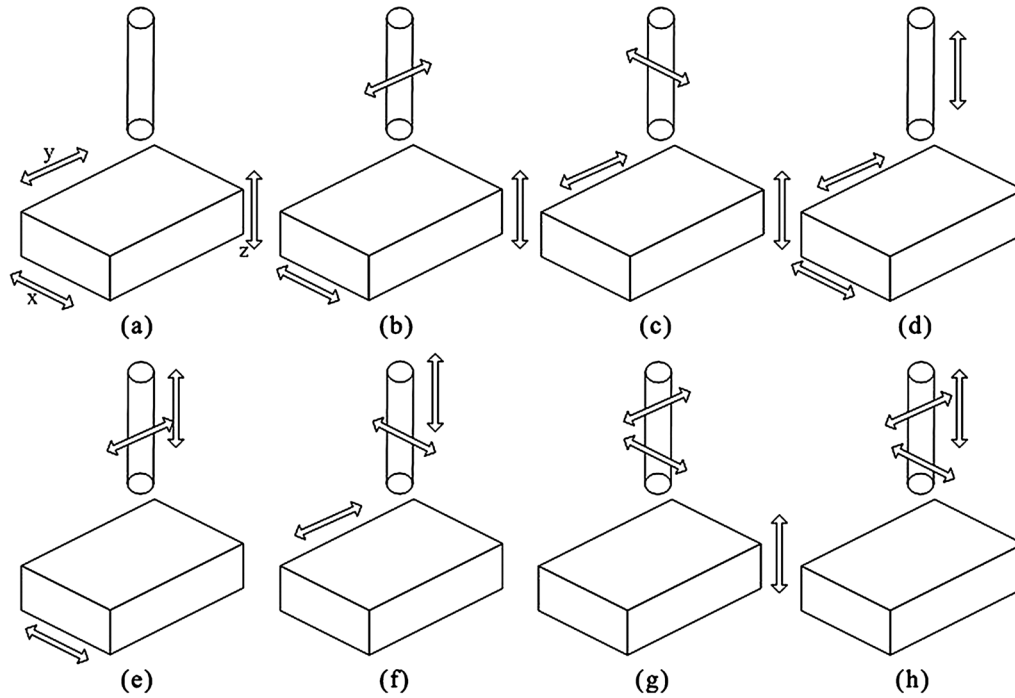


Fig. 2 Eight types of movement layout for linear 3-D motion.

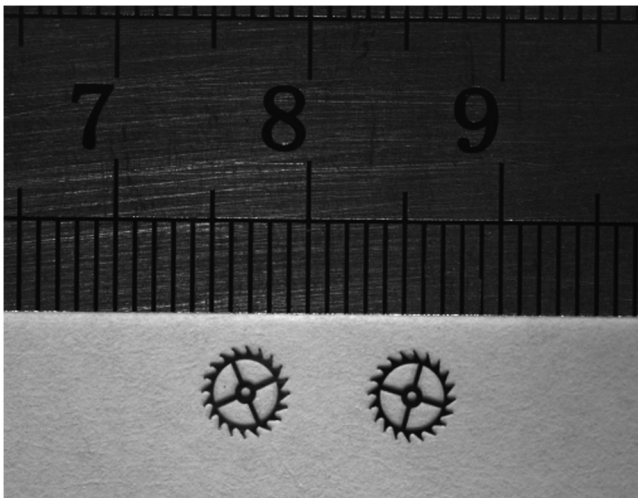


Fig. 3 Escape wheel.

component and the workbench must be small enough to obtain an undistorted image.¹³ As shown in Fig. 4, the line AB represents that the theoretical object plane perpendicular to the optical axis, while the line AB' represents the tilted situation with the radial error σ_x caused by the deviation angle ϕ . The lengths of both AB and AB' are equal to 7.4 mm. To capture an undistorted image, σ_x must be less than $3 \mu\text{m}$, the accuracy for the watch escapement; and the allowed deviation angle will be less than 1.63 deg by Eq. (1). Such a precision is not too high to be realized in a measuring instrument.

$$\sigma_x = AB - AB' \cos \phi = AB(1 - \cos \phi) \quad (1)$$

$$\sigma_z = AB \cdot \sin \phi. \quad (2)$$

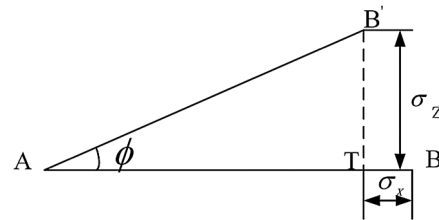


Fig. 4 The position between optical axis and object plane.

However, a higher demand on perpendicularity is required by further analysis of defocus effects caused by the vertical deviation angle.^{14,15} When ϕ approaches 1.63 deg, σ_z will be about $210.5 \mu\text{m}$ by Eq. (2). It is far beyond the allowed depth of field and will cause the image to be blurred. In fact, σ_z has to be limited to $\pm 10 \mu\text{m}$ to meet the requirement of depth of field. And meanwhile, ϕ needs to be less than 0.155 deg, which is somewhat difficult to realize.

Note that there is a perpendicularity change as long as the vertical trajectory is not just along the z -axis, no matter if the workbench or the shooting device is used to accomplish z -axis movement. In the VIIWE, there are only two cases for feeding vertically involving a calibration of perpendicularity (see Sec. 5), switching to workpieces with different thickness; and the ranges of both cases are below 0.3 mm. For this reason, we choose a precise lift bench, Seiki B33-80 (Suruga, Shizuoka, Japan) with a dimension of $80 \times 80 \text{ mm}^2$, as a power source in the vertical movement. The parallelism error of the upper surface relative to the original plane is less than $5 \mu\text{m}$, and the straightness error in vertical motion is less than $3 \mu\text{m}$. Figure 5(a) and 5(b) shows the shooting device and the workbench as a z -axis movement unit separately. Here, T , S and P represent the length of z -axis feeding, the straightness of the lift, and

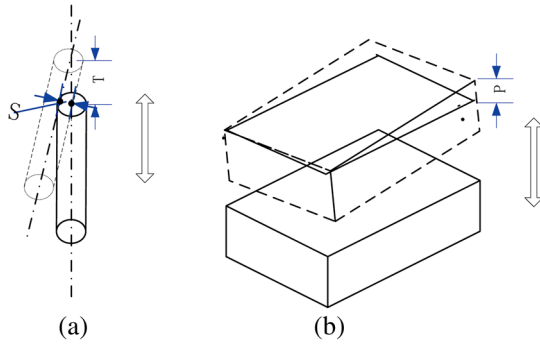


Fig. 5 The impact on perpendicularity caused by Z-axis movement.

the maximum value of the surface's parallelism, respectively. According to the theory of triangle, the vertical deviation angle in Fig. 5(a) can reach 0.573 deg, which is beyond the limit of vertical deviation angle. The deviation angle in Fig. 5(b) is only 0.003 deg, which has less influence on measurement results. Therefore, with workbench acting as the movement layout along the z-axis, the movement layout form in Fig. 2(g) will be better than the one in Fig. 2(h) for its benefit of the perpendicularity.

3.2 Parallelism Analysis

Indeed, the deviation of perpendicularity affects the error of object distance partially, while the deviation of parallelism between probe movement plane and workbench will affect the object distance in the entire workbench.¹⁶ As shown in Fig. 6, O - XYZ and o - xyz represent the coordinate systems of the moving camera and the still workbench respectively. If the plane YOX is not parallel to the plane yox , the object distance error will be introduced. To meet the requirements of depth of field, we have to keep the prerequisites below. The linear parallelism error between the line OX/OY and the line ox/oy is kept less than 20 μm per 100 mm. The plane parallelism error between the plane OXY and the plane oxy is less than 50 μm in the entire measuring range.

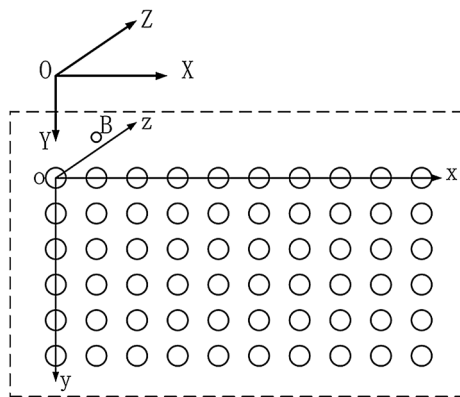


Fig. 6 The moving camera and the still workbench coordinate systems.

4 Adjustment for Perpendicularity and Parallelism

It is hard to keep both parallelism and perpendicularity stable because of the strict requirements for the two parameters and the continuous movement of the shooting component when the parts are being measured. Thus, proper methods should be provided to quantify and correct the errors. Unlike many manufacturers who use other high-accuracy devices to calibrate and adjust these two parameters, we design a specialized adjustment scheme for VIIWE for the convenience of users.

4.1 Perpendicularity Adjustment

The adjustment mechanism about perpendicularity is the carrier of the shooting component. As shown in Fig. 7, the coordinate system is composed of the optical axis $O'Z$ and two movement axes $O'X$ and $O'Y$. Both lens and camera are fixed on the plate 1 that is held by plate 2. The rational perpendicularity of the optical axis to workbench can be obtained by adjusting the plate 2 in the X - Z plane and Y - Z plane. The adjustments in both planes rely on the rotational motion, and the two axes of rotations intersect at the point O where a pivot pin in a hole is adopted to play the role of the axes in practice. In the X - Z plane, the plate 2 is forced to rotate left or right by two long screws marked C and D in Fig. 7, which are installed in both sides of plate 1, while in Y - Z plane, the plate 2 rotates backward or forward by the frontal screws marked A and B in Fig. 7 extruding two flexible gaskets. After adjusting, three inner-hexangular bolts marked as N , P , and M in Fig. 7 fasten plate 1 tightly and keep the perpendicularity stable in case the adjusted screws become loose.

In the design of structure, the rotation radius is 180 mm in the X - Z plane and 185 mm in the Y - Z plane. Thin-tooth M5 screws are chosen as the adjusting knobs with a thread pitch of 0.5 mm. Therefore, the adjustment precision ζ can be calculated when turning the screw for one cycle.

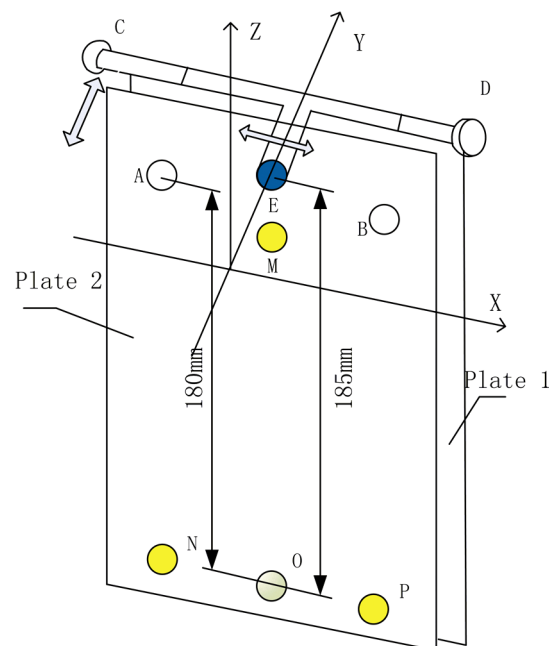


Fig. 7 The adjustment mechanism for perpendicularity.

In the X-Z plane:

$$\zeta_1 = \frac{180}{\pi} \frac{B}{R_1} = 0.159 \text{ deg} = 9.6' \quad (3)$$

In the Y-Z plane:

$$\zeta_2 = \frac{180}{\pi} \frac{B}{R_2} = 0.155 \text{ deg} = 9.3' \quad (4)$$

In order to quantify the amount of adjustment for these four screws, the perpendicularity is calculated with a regional definition, developed and achieved by a PC with its basic principles summarized as follows. If a deviation angle between the axis of the shooting component and a measured standard model exists, the definition that can be measured by the gray scale contrast with image processing technologies will be different in four different regions of the model. Therefore, the perpendicularity of the machine can be self-calibrated with only one standard model. The amount of screw adjustment can be calculated by Eq. (5).

$$\begin{bmatrix} x_A & x_B & x_C & x_D \end{bmatrix} = \begin{bmatrix} \zeta_1^{-1} & 0 & 0 & 0 \\ 0 & \zeta_1^{-1} & 0 & 0 \\ 0 & 0 & \zeta_2^{-1} & 0 \\ 0 & 0 & 0 & -\zeta_2^{-1} \end{bmatrix} \begin{bmatrix} y_A \\ y_B \\ y_C \\ y_D \end{bmatrix} \quad (5)$$

4.2 Parallelism Adjustment

In this equipment, we divide a “plane to plane” parallelism adjustment into two orthogonal “line to plane” parallelism adjustments each with the same basic principles. Not only can the screws shown in Fig. 8 fix the marble platform to the table, but they can also adjust the “line to plane” parallelism. Screw 2 is ordinary, and screw 3 has the same tooth as those used in perpendicularity adjustment. In the initial state, the preload of screw 2 is small. The marble platform can be rotated clockwise and anticlockwise by turning screw 1 or screw 3. Tightening screw 2 can increase preload to keep the platform stable.

In the testing process, a dial indicator that is mounted on the moving shooting component touches the upper surface of the workbench to calibrate parallelism. It should not stop

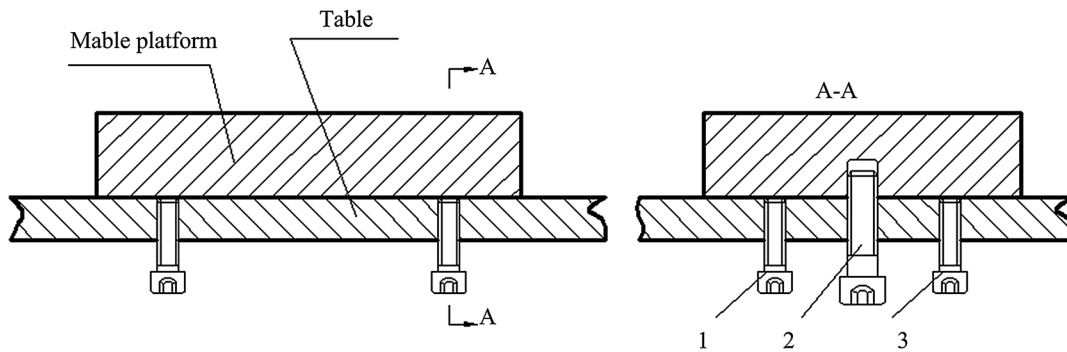


Fig. 8 Parallelism adjustment sketch.

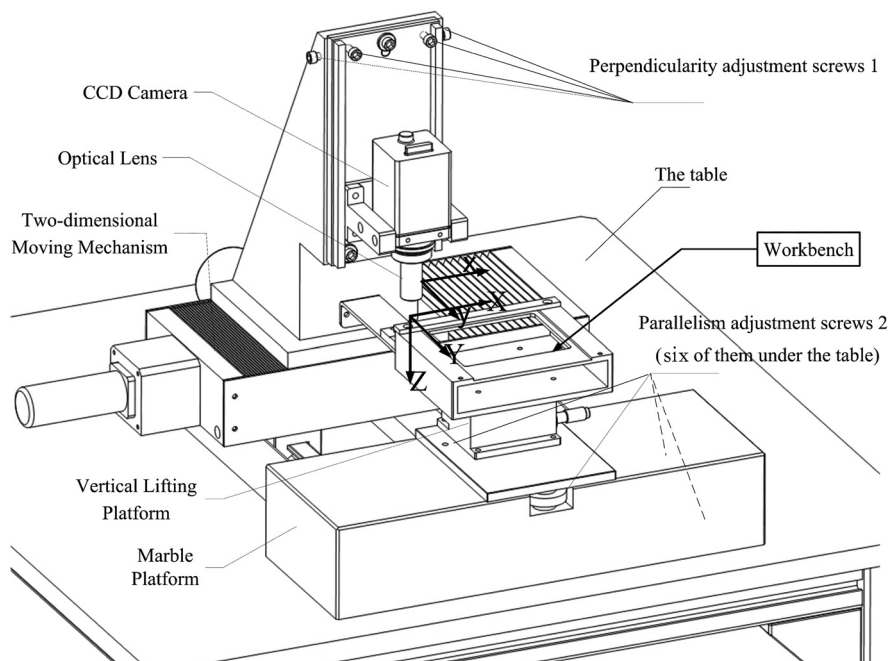


Fig. 9 Main structure of VIIWE.

adjusting the screws until all values the dial indicator shows are very close to each other. The disadvantage of this method is that the amounts of adjustment for the screws could not be calculated quantitatively by Eq. (6) because its accuracy also relates to the unknown preload of the screw 2. However, the following equation will be useful when the parallelism is adjusted iteratively.

$$[x_m \ x_n] = \frac{1}{\zeta} [y_m \ y_n]. \tag{6}$$

5 Results

Figure 9 shows the concrete structure of the VIIWE. In the layout, a two-dimensional movement mechanism and a lifting bench are used to drive the shooting device to move in three-dimensional space. For the adjustment, the screws 1 and the screws 2 are responsible for the parallelism and the perpendicularity respectively.

There are two main phases in the adjustment flow chart as shown in Fig. 10. Phase 1 is to compute deviation angles of parallelism and adjust them, and phase 2 is responsible for

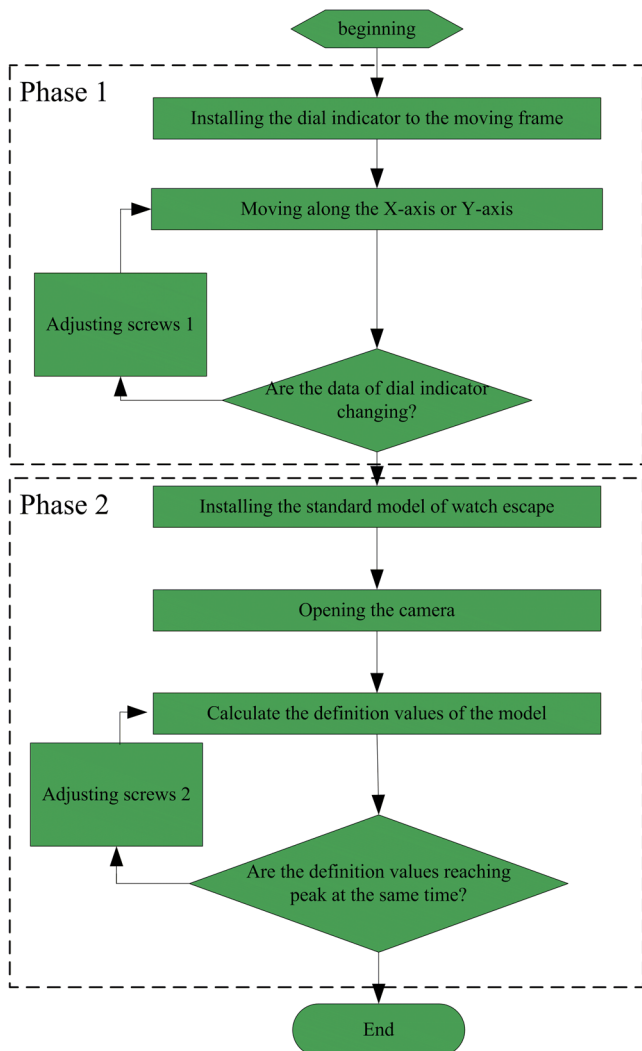


Fig. 10 The adjustment flow chart.

the perpendicularity. Both the perpendicularity and parallelism adjustments are not very complicated.

As the deviation angles of parallelism and perpendicularity are both adjusted by the same jiggle screw structure, we only verify the effect of perpendicularity adjustment scheme here. There are four symmetrical regions at two coordinate axes of a standard model with the size of $7.4 \times 7.4 \text{ mm}^2$. Adimec4000C (EA, Eindhoven, The Netherlands), a high resolution digital camera, is utilized to capture the image of the four regions simultaneously. The regional definitions are calculated by the gradient square function¹⁷ as shown in Table 1. The distance between each two adjacent positions is $10 \mu\text{m}$. Region A in position 8, region B in position 11, region C in position 2, and region D in position 5 reach their maximum. In other words, the vertical deviations are $(8 - 2) \times 10 \mu\text{m}$ in the X-Z plane and $(11 - 5) \times 10 \mu\text{m}$

Table 1 Experimental data before adjustment.

Position	Value: Region			
	A	B	C	D
1	7574	6487	5839	6852
2	7777	6719	5878*	6998
3	8566	7912	5698	7488
4	8653	8159	5620	7529
5	8740	8397	5524	7549*
6	8784	8604	5435	7546
7	8798	8787	5327	7522
8	8791*	8978	5223	7476
9	8751	9139	5098	7406
10	8355	9515	4607	6980
11	8217	9532*	4485	6846
12	8050	9511	4357	6084

*The maximal value in a region

Table 2 Experimental data after adjustment.

Position	Value: Region			
	A	B	C	D
1	6617	7872	5153	6798
2	6680	7944	5183	6855
3	6714	7997	5207	6890
4	6733*	8020*	5215*	6904*
5	6730	8008	5211	6899

*The maximal value in a region

in the Y - Z plane. Meanwhile, the deviation angles both in the X - Z plane and in the Y - Z plane reach 0.465 deg by Eq. (2). The two frontal ones of the screws 4 are rotated clockwise for three circles and the two side ones anticlockwise for 2.9 cycles by the following the equation:

$$n = \Phi/\zeta. \quad (7)$$

The values of regional definitions retested after adjustment are shown in Table 2. The values in four regions reach the maximum at the same position, i.e., the workbench and the optical axis are vertical to each other. The results prove that this procedure is linear, precise, and effective to adjust the perpendicularity of VIIWE.

6 Conclusion

This paper presented a scheme of movement layout and adjustment in design of SVMS with an example of the VIIWE. Two requirements in the VIIWE were placing the watch escapements freely and regularly, capturing a single image entirely with a small depth of field lens. First, the forms of movement layout of the SVMS were discussed, and an optimized one for the VIIWE was chosen. Second, an adjustment scheme was introduced after analyzing the influences on image sharpness caused by parallelism and perpendicularity. The movement layout we chosen not only met the requirements of placing the watch escapements, but also benefited the perpendicularity of the VIIWE. The precision of the adjustment mechanism could be better than $10'$, which enabled us to keep the workpieces within a small depth of field all the way. Our method is intuitive and useful for other SVMS designs.

Acknowledgments

This project is funded by Major Science and Technology Funded Project of National High-grad CNC (2009ZX04014-092) and Research on the Automatic Flexible Measurement and Automatic Separation Technology (NO. 09JCZDJC26700).

References

1. F. Mason, "Video measurement," *Qual. Manuf.* **24**(11), 11–12 (2001).
2. Z. Wang and Z. W. Wang, "Semi-automatic inspecting instrument for watch escape wheel based on machine vision," *Seventh International Symposium on Precision Engineering Measurements and Instrumentation*, Lijiang, China (2011).
3. S. Leslie, *View Camera Technique*, 3rd ed., pp. 136–139, Focal Press, London (1976).
4. J. Zhang et al., "Verticality detection algorithm based on local image sharpness criterion," *Chin. J. Mech. Eng.* **25**(1), 173–178 (2012).
5. S. Y. Chen and Y. F. Li, "Automatic sensor placement for model-based robot vision," *IEEE Trans. Syst. Man Cybern. B*, **34**(1), 393–408 (2004).
6. W. R. Scott, "Model-based view planning," *Mach. Vis. Appl.* **20**(1), 47–69 (2009).
7. J. R. Ryoo and T. Y. Doh, "Auto-adjustment of the objective lens neutral position in optical disc drives," *IEEE Trans. Consum. Electr.* **53**(4), 1463–1468 (2007).
8. K. Yokoyama et al., "Optical beam deflection noncontact atomic force microscope optimized with three-dimensional beam adjustment mechanism," *Rev. Sci. Instrum.* **71**(1), 128–132 (2000).
9. Optical instrument design manual editing group, *Optics Design and Optics Measurement*, pp. 537–544, Mechanical Industry Press, China (1971).

10. A. L. Wang et al., *Modern CN Machine*, pp. 281–296, National Defense Industry Press, China (2005).
11. J. Zhang et al., "Super-resolution reconstruction of image in high accuracy image measuring system," *Opt. Precis. Eng.* **19**(1), 168–174 (2011).
12. E. Goron et al., "Original 3D feeding structures for enhancing micro-strip antennas operating bandwidth," in *35th Microwave Conference*, Paris, France (4–6 Oct. 2005).
13. H. Gong et al., "A method of verticality adjusting between optical axis and carrier in two-dimensional vision measurement," *J. Beijing Inform. Sci. Technol. Univ.* **21**(3), 35–38 (2006).
14. T. Y. Yu and H. Y. Tan, *Engineering Optics*, pp. 58–63, Mechanical Industry Press, Beijing (2002).
15. W. J. Smith, "Aberrations" Chapter 3, in *Modern Optical Engineering*, pp. 71–72, SPIE Press McGraw-Hill, Bellingham, Washington, USA (2000).
16. G. Sansoni, P. Bellandi, and F. Docchio, "Design and development of a 3D system for the measurement of tube eccentricity," *Meas. Sci. Technol.* **22**(7), 1–12 (2011).
17. J. J. Zhao, R. L. Bai, and D. Li, "A new method of verticality adjusting between optical axis and object surface of embedded machine vision controller," *Optoelectr. Eng.* **37**(5), 63–69 (2010).



Xinbo Liu received his master's degree from Tianjin University in 2007. Now he is studying in the College of Precision Instrument and Opto-electronics Engineering of Tianjin University as a PhD candidate. His main research interests are precision measurement and machine-tool calibration.



Zhong Wang gained his master's degree from Tianjin University in 1991. Now he is a professor of Tianjin University in China. His main research interests are precision measurement, instrument intelligence, micro-accessory measurement technology based on full imaging and on-time detection, and classification technology in industry.



Jigui Zhu, PhD, is a professor at Tianjin University in China. He is an expert in laser and opto-electric detection, and visual inspection.



Jin Zhang received his PhD in instrument science and technology from Tianjin University in 2010. Presently, he is a lecturer at Hefei University of Technology, working on data traffic technology, precision measurement, and instrument intelligence.